RESEARCH ARTICLE

EFFECT OF TiO₂ AS AN ELECTRON TRANSPORT LAYER ON P3HT:IC70BA ORGANIC SOLAR CELL

*,1,2Mervat K. Tameem and 1Bushrah A. Hassan

[1]Physics Department, College of Science, Baghdad University, Baghdad, Iraq
[2]Optics Techniques Department, Dijlah University College, Baghdad, Iraq

ABSTRACT

A cathode buffer layer made of TiO₂ introduced in poly(3-hexylthiophene) (P3HT): Indene-C70 Bis-Adduct (ICBA) bulk heterojunction (BHJ) solar cell. The open-circuit voltage and fill factor increase respectively to 0.62 V and 63%, due to the enhanced electron extraction by inserting a TiO₂ layer between the active layer and Al cathode. Thus, the power conversion efficiency increases from 5.8 % to 8% and the ecofriendly permanency is also much enhanced.

INTRODUCTION

Bulk heterojunction (BHJ) polymer solar cells (PSCs) have attracted considerable attentions in both academia and industry due to their low cost, flexibility and large-area fabrication features (Yip and Jen, 2012; Hoppe and Sariciftci, 2004; Cai et al., 2010) compared to traditional SCs (Kosten et al., 2013; Su et al., 2012; Taylor, 2012). Although the power conversion efficiency (PCE) of 9.2% has been reported for single BHJ PSCs (He et al., 2012), the efficiency is still lower than their inorganic semiconductor counterparts owing to the narrow absorption spectrum of polymer semiconductor (Jo et al., 2013; Krebs, 2009; Ameri et al., 2013). In the past few years, research efforts have focused on the developing highly efficient PSCs through various methods, such as polymer synthesis (He et al., 2011; Cheng et al., 2013), interfacial control (Intemann et al., 2014; Zou et al., 2014), tandem device (Dou et al., 2012). Some light management method (Chen et al., 2013; Guo et al., 2014; Holman et al., 2013; Lai et al., 2013; Romano et al., 2014; Huang et al., 2013), including microcavity, photon crystal and surface Plasmon have also been applied to enhance light absorption. Since the electrical contacts between the active layer and electrodes are determinative for efficient charge transport and extraction, the interfacial control plays an

especially important role in the PCE (Po et al., 2011; Chen et al., 2009). The most typical OPV structure is based on the bulk heterojunction (BHJ) concept, in which a polymeric electron donor and a fullerene based electron acceptor are mixed in solution and cast into a thin film that is sandwiched between two electrodes (Dennler et al., 2009). The efficiency of the BHJ is restricted by the random network that is formed through the coating and drying of the photoactive solution due to phase segregation kinetics. This leads to the formation of dead ends and isolated domains that trap charge carriers and prevent them from being extracted (Yang and Loos, 2007). Additionally, due to the low mobility of BHJ materials, there is rivalry between the dissociation and the recombination of the photo generated carriers within the thin BHJ film (Blom et al., 2007). The PCE of the PSCs based on P3HT:PCBM reached over 4% (Ma et al., 2005; Li et al., 2005; Reyes-Reyes et al., 2005) by thermal treatment (Ma et al., 2005), solvent (Li et al., 2005) and vapor (Zhao et al., 2007) annealing, as well as mixture solvent treatment. However, further improvement of the photo voltaic performance of the PSCs based on P3HT:PCBM is limited because of the relatively small energy difference between the low estunoccupied molecular or bital (LUMO) of PCBM and the highest occupied molecular orbital (HOMO) of P3HT, which results in a lower open circuit voltage (Voc) of the P3HT:PCBM based PSCsto -0.6 V. In order to further improve device performance, anovelindene-C60 bisadduct (ICBA) (He et al., 2010; Zhao et al., 2010; Cheng et al., 2010; Chang et al., 2011) with a higher LUMO

*Corresponding author: Mervat K. Tameem
Physics Department, College of Science, Baghdad University, Baghdad, Iraq.

energy level of -3.74 eV which is higher than that of PCBM was employed as photovoltaic electron acceptor with matching up P3HT as photovoltaic electron donor. Obviously, it will results in a higher Voc and PCE of the P3HT:ICBA based PSCs than that of the P3HT:PCBM based PSCs because of the ICBA with a higher LUMO energy level. The interface modification on polymer active layer/electrodes has been comprehensively carried out for the improvement of charge injection or collection, especially due to mismatched energy level between polymer materials and metal electrodes (Zhao *et al*., 2010; Yang *et al*., 2008; Peumans *et al*., 2003; Benor *et al*., 2010; Kim *et al*., 2010; J¨onsson *et al*., 2005). In order to modify the interface between active layer/ electrodes, many buffer layers or ultrathin layer have been reported, such as hole collecting buffer layers containing poly (3,4-ethylenedioxythiophene): poly (styrenesulfonate) (PEDOT: PSS) (Benor *et al*., 2010; Kim *et al*., 2010), MoO_3 (Cheng *et al*., 2011; Zhang *et al*., 2010), WO_3 (Yongbing, 2010), V_2O_5 (Espinosa *et al*., 2011), and electron collecting buffer layers containing $CsCO_3$ (Chen *et al*., 2008), TiO_2 (Baek *et al*., 2009), LiF (J¨onsson *et al*., 2005; Ahlswede *et al*., 2007; Gao *et al*., 2010; Brabec *et al*., 2002), Ca (Zhang *et al*., 2010), ands as to improve the device performance. However, the operation mechanism of these buffer or ultrathin layers is still in debate. Forming a tunneling junction to increase built-in electric field, an interfacial dipole layer to shift the work function of electrodes, ortoprotect the active layer from damage is considered the under lying reason (Cai *et al*., 2010). In this paper, we explored the enhanced performance of P3HT:ICBA based polymer solar cellsusing TiO_2 asan electron collecting buffer layer and PEDOT:PSS as a hole collecting buffer layer.

MATERIALS AND METHODS

OPVs were fabricated using pre-patterned ITO-coated glass substrate. Prior to the use, the substrate was cleaned in ultrasonic using 20% Decon90, deionized water, isopropanol, and acetone in the clean room, and later dried with N_2 compressor. All cleaned substrates were treated with O_2 plasma treatment for 25 min. The solution for hole transporter PEDOT:PSS solution was spin-coated at 5000 rpm for 40 s onto the cleaned substrates and annealed at 140 °C for 10 min. The photoactive layer P3HT:ICBA (1:1) w dissolved in Chlorobenzene with a concentration of 15mg/ ml was spin-coated at 1500 rpm for 35 s in the glove box and annealed at 170 °C for 45 min. Later, TiO_2 solution was spin-coated at 4000 rpm for 25 s onto the photoactive layer and annealed at 75 °C for 25 min. To complete the device, 120 nm thick Al was thermally evaporated at rate 1A/s through a shadow mask at a base pressure of 10^{-6} mbar. The active area of the complete devices is 0.12 cm². Devices were tested under AM 1.5 illumination with an intensity of 100 mW/cm² simulator at room temperature. The idealized device configuration is illustrated in Fig. 1.

RESULTS AND DISCUSSION

Surface Morphology

In order to get a complete sight of comparison between both structures, an Atomic Force Microscopy (AFM) was used to examine the TiO_2 films on top of the active layer, before the back electrode deposition. The topographies are shown in

Figure 2. For pristine TiO_2 films cast from as-diluted solutions (as described in materials synthesis), the root mean square (RMS) roughness were 13.4 nm for TiO_2, while for active layer without using TiO_2 the (RMS) was 25.5 nm. Films made with TiO_2 composites show a lower roughness compared to those without it.
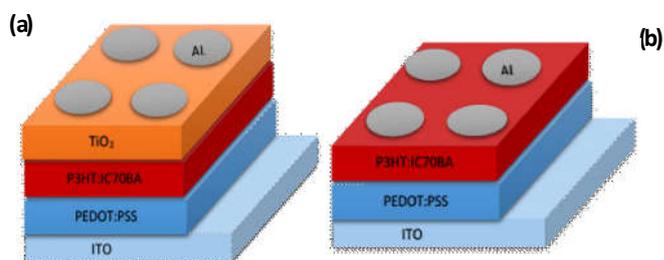
Fig. 1. Schematic diagram of P3HT:IC70BA based OBHJ solar cells (a) with TiO₂ (ETL) layer and (b) without TiO₂ (ETL) layer
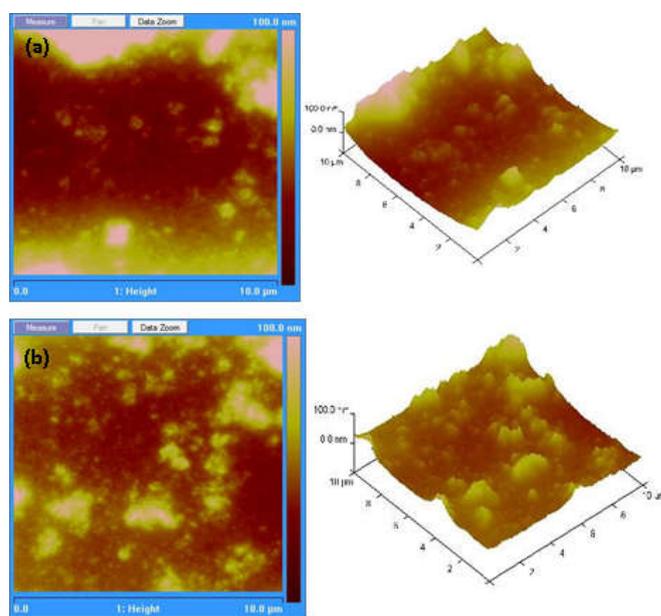
Fig. 2. AFM topography images of (a) P3HT:IC70BA on ITO/PEDOT:PSS and (b) TiO₂ on P3HT:IC70BA on ITO/PEDOT:PSS

Optical Characterization

The absorption spectra for devices of the same architecture with and without TiO_2 as ETLs are shown in Figure 3. The absorption spectra are very similar for both devices indicating there is minimum absorption from the ETLs; this suggests that it does not interfere with the ETL's secondary function as an optical spacer. (Ma *et al*., 2002; Shrotriya *et al*., 2006) As a result, the enhanced efficiencies observed with the TiO_2 hybrid ETLs can be ascribed primarily to their improved electrical characteristics. The optical energy gap values (E_g^{opt}) for P3HT:ICBA blends with and without TiO_2 as an electron transport layer are shown in Fig. 4. This figure reveals that the values of direct optical energy gap with TiO_2 exceeded that without TiO_2 because there is blue shift absorbance. On the other hand, the extinction coefficient and the refractive index reduced for devices usingTiO_2 buffer layer as shown in Fig. 5 and 6.Table (1)exhibited the optical constants at λ=700 nm for P3HT:ICBA OBHJ devices with and without TiO_2 ETL.
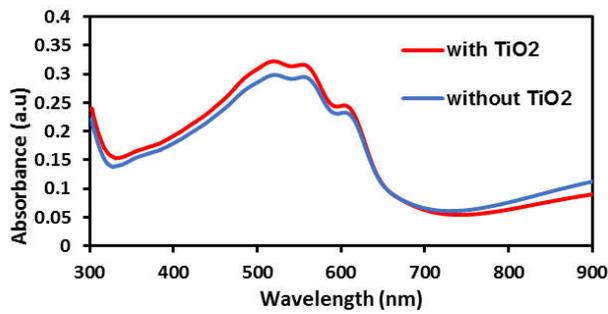
Fig. 3. UV-visible absorbance for devices with and without TiO₂ ETL
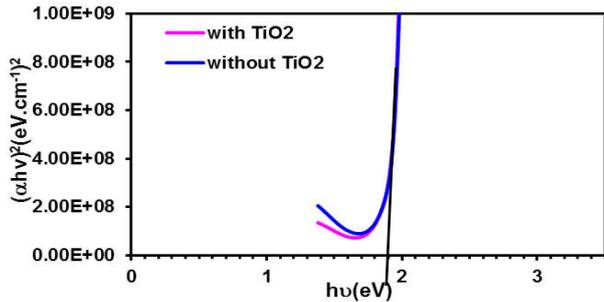
Fig. 4. Variation of (αhυ)² versus the photon energy (hυ) for P3HT:IC70BA OBHJ devices with and without TiO₂ ETL
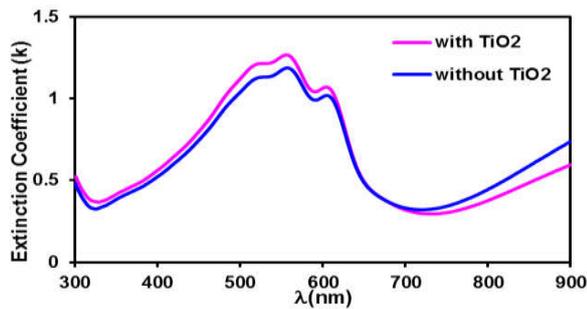
Fig. 5. Variation of extinction coefficient (k) with wavelength for P3HT:IC70BA OBHJ devices with and without TiO₂ ETL
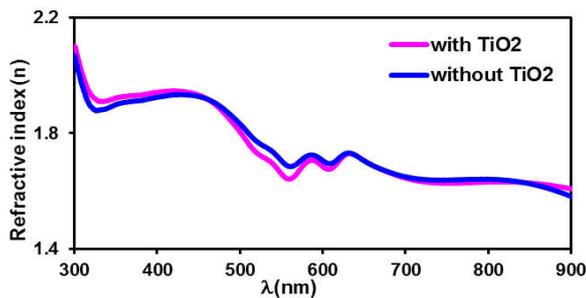
Fig. 6. Variation of Refractive Index (n) with wavelength for P3HT:IC70BA OBHJ devices with and without TiO₂ ETL

Table 1. Optical constants at λ=700 nm for P3HT:ICBA OBHJ devices with and without TiO₂ ETL

Device	A (a.u)	E_g (eV)	k	n
With TiO₂	0.05	1.91	0.30	1.63
Without TiO₂	0.06	1.90	0.34	1.64

Electrical Characterization

The current density–voltage (J–V) characteristics under AM 1.5G one-sun illumination condition is shown in Figure 7. Table (2) summarizes the characteristics of the device performance with and without TiO₂. A comparison of devices with an Al electrode to those with a TiO₂/Al electrode shows that the insertion of a TiO₂ layer between the active layer and the evaporated Al cathode layer leads to a significant improvement in device performance. It is known that the open circuit voltage is generally determined by the difference between the highest occupied molecular orbital (HOMO) of the donor and the lowest unoccupied molecular orbital (LUMO) of the acceptor in the case of an Ohmic contact between the active layer and the cathode (Brabec *et al*., 2001). Thus, the increase in V_{oc} may arise from the work function of TiO₂. The V_{oc} increases from 0.36 V (for the device with no interlayer) to 0.62 V and the FF improves dramatically up to 63%. This yields to a high power conversion efficiency (PCE) of 8%. As a result, TiO₂ is a promising candidate for using as an interfacial layer, as it has been shown that inorganic oxides are quite stable to oxygen and moisture (Butterworth *et al*., 1995). One possible reason for the increased performance of the devices with TiO₂ is the formation of a better Ohmic contact that is created by the decreased conduction band level of the TiO₂ such that the interfacial layer facilitates electron transport from the active layer to the cathode. The serial resistance is slightly decreased from 2.7–2.1 Ω, while the shunt resistance remains as high as 31.64 Ω, making it ideal for photovoltaics. The ideality factor β as shown in Table (2) is slightly increased with the insertion of buffer layer due to the increasing of the structural defects. It is believed that the TiO₂ layer can keep the hot Al electrode from diffusing into the active layer during evaporation and can offer good contact morphology between the active layer and the electrode.
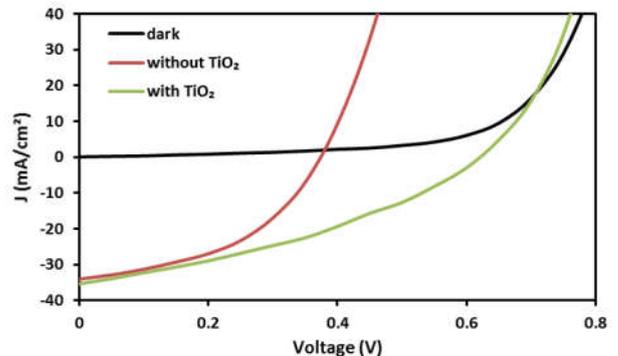
Fig. 7. J-V characteristics of the OBHJ solar cells with and without TiO₂ under the illumination of 100 mW/cm² white light
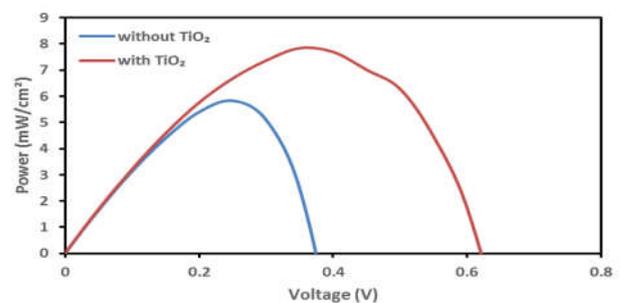
Fig. 8. Power curve of P3HT:IC70BA bulk devices with and without TiO₂ interfacial layer
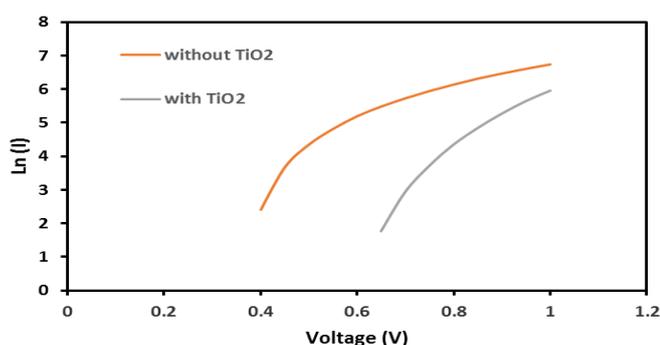
Fig. 9. Variation of Ln(I) versus the bias voltage for P3HT:IC70BA OPV devices with and without TiO$_2$ interfacial layer

Table 2. The extracted and calculated photovoltaic parameters of the fabricated devices

Device	V_{oc} (V)	J_{sc} (mA/cm^2)	FF (%)	PCE (%)	$R_s\ \Omega$	$R_{sh}\ \Omega$	β
Without TiO$_2$	0. 36	34.08	27.6	5.83	2.7	40	1.52
With TiO$_2$	0.62	35.25	63	8	2.1	31.64	1.65

Conclusion

The effect of TiO$_2$ interlayer on the P3HT:IC70BA BHJ solar cell was studied. Inserting TiO$_2$ layer between the active layer and Al cathode decreases the work function of cathode and reduces the series resistance. Therefore, Voc increases from 0.36 to 0.62 V, FF increases from 27.6% to 63% and significantly increment in PCE from 5.83% to 8%. Note that short circuit current density Jsc is almost the same. Besides of the above, the insertion of TiO$_2$layer prevent the Al atoms from diffusion into the active layer and thus improve the lifetime of BHJ cells.

REFERENCES

Ahlswede E., J. Hanisch, M. Powalla, 2007. Comparative study of the influence of LiF, NaF, and KF on the performance of polymer bulk heterojunction solar cells, *Applied Physics Letters*, 90: 163504.

Ameri, T., N. Li, C.J. Brabec, 2013. Highly efficient organic tandem solar cells: a follow up review, *Energy Environ. Sci.*, 6: 2390–2413.

Baek W., I. Seo, T. Yoon, H. Lee, C. Yun, Y. Kim, 2009. Hybrid inverted bulk heterojunction solar cells with nanoimprinted TiO$_2$ nanopores, *Solar Energy Materials and Solar Cells*, 93:1587–1591.

Benor A., S.-Y. Takizawa, C. Pe´ rez-Bolı´var, P. Anzenbacher Jr, 2010. Efficiency improvement of fluorescent OLEDs by tuning the working function of PEDOT:PSS using UV–ozone exposure, *Organic Electronics*, 11: 938–945.

Blom, PWM., VD Mihailetchi, LJA Koster, DE Markov. 2007. Device physics of polymer: fullerene bulk heterojunction solar cells. *Adv Mater.*, 19:1551–66.

Brabec C. , S. Shaheen C. Winder N. Sariciftci P. Denk, 2002. Effect of LiF/metal electrodes on the performance of plastic solar cells, *Applied Physics Letters*, 80:1288–1290.

Brabec C. J., A. Cravino, D. Meissner, N. S. Sariciftci, T. Fromherz, M. T. Rispens, L. Sanchez, J. C. Hummelen,

2001. Origin of the Open Circuit Voltage of Plastic Solar Cells, *Adv. Funct. Mate*r., 11, 374.

Butterworth, M., R. Corradi, J. Johal, S. Lascelles, S. Maeda, S. Armes, 1995. Zeta potential measurements on conducting polymer-inorganic oxide nanocomposite particles, *J. Colloid Interf. Sci.*, 174, 510.

Cai, W., X. Gong, Y. Cao, 2010. Polymer solar cells: Recent development and possible routes for improvement in the performance, *Solar Energy Materials and Solar Cells*, 94:114–127.

Cai, W., X. Gong, Y. Cao, Polymer solar cells: recent development and possible routes for improvement in the performance, *Sol. Energy Mater. Sol.*, Cells 94 (2010) 114–127.

Chang C., C. Wu, S. Chen, C. Cui, Y. Cheng, C. Hsu, Y. Wang, Y. Li, 2011. Enhanced performance and stability of a polymer solar cell by incorporation of vertically aligned, cross-linked fullerene nanorods, *Angewandte Chemie International Edition England*, 50:9386–9390.

Chen F., J. Wu, S. Yang, K. Hsieh, W. Chen, 2008. Cesium carbonate as a functional inter layer for polymer photovoltaic devices, *Journal of Applied Physics*, 103: 103721–103725.

Chen H., J. Hou, S. Zhang, Y. Liang, G. Yang, Y. Yang, L. Yu, Y. Wu, G. Li, 2009. Polymer solar cells with enhanced open-circuit voltage and efficiency, Nat. Photonics 3: 649–653.

Chen, X., B. Jia, Y. Zhang, M. Gu, 2013. Exceeding the limit of plasmonic light trapping in textured screen-printed solar cells using Al nanoparticles and wrinkle-like graphene sheets, *Light Sci. Appl.*, 2: e92-1–e92-6.

Cheng F., G. Fang, X. Fan, H. Huang, Q. Zheng, P. Qin, H. Lei, Y. Li, 2013. Enhancing the performance of P3HT:ICBA based polymer solar cells using LiF as electron collecting buffer layer and UV-ozone treated MoO3 as hole collecting buffer layer, Sol. Energy Mater. Sol. Cells 110: 63–68.

Cheng F., G. Fang, X. Fan, N. Liu, N. Sun, P. Qin, Q. Zheng, J. Wan, X. Zhao, 2011. Enhancing the short-circuit current and efficiency of organic solar cells using MoO$_3$ and CuPc as buffer layers, *Solar Energy Materials and Solar Cells*, 95: 2914–2919.

Cheng Y. , C. Hsieh, Y. He, C. Hsu, Y. Li, 2010. Combination of indene-C60 bis-adduct and cross-linked fullerene interlayer leading to highly efficient inverted polymer solar cells, *Journal of the American Chemical Society,* 132: 17381–17383.

Dennler G, Scharber MC, Brabec CJ. 2009. Polymer–fullerene bulk heterojunction solar cells. *Adv Mater.*, 21:1323–38.

Dou L., J. You, J. Yang, C.-C. Chen, Y. He, S. Murase, T. Moriarty, K. Emery, G. Li, Y. Yang, 2012. Tandem polymer solar cells featuring a spectrally matched low-bandgap polymer, *Nat. Photonics*, 6:180–185.

Espinosa N., H. F. Dam, D. M. Tanenbaum, J. W. Andreasen, M. Jørgensen, F. C. Krebs, 2011. Roll-to-roll processing of inverted polymer solar cells using hydrated vanadium(V) oxide as a PEDOT:PSS replacement, Materials 4: 169–182.

Gao D., M. G. Helander, Z. B. Wang, D. P. Puzzo, M. T. Greiner, Z. H. Lu, 2010. C60: LiF blocking layer for environmentally stable bulk heterojunction solar cells, Advanced Materials 22:5404–5408.

Guo, C., T. Sun, F. Cao, Q. Liu, Z. Ren, 2014. Metallic nanostructures for light trapping in energy-harvesting devices, Light Sci. Appl. 3: e161-1–e161-12.

He Y., H. Chen, J. Hou, J. Li, 2010. Indene C60 bisadduct: a new acceptor for high-performance polymer solar cells, Journal of the American Chemical Society 132: 1377–1382.

He Z., C. Zhong, X. Huang, W.Y. Wong, H. Wu, L. Chen, S. Su, Y. Cao, 2011. Simultaneous enhancement of open-circuit voltage short-circuit current density and fill factor in polymer solar cells, Adv. Mater. 23: 4636–4643.

He, Z., C. Zhong, S. Su, M. Xu, H. Wu, Y. Cao, 2012. Enhanced power-conversion efficiency in polymer solar cells using an inverted device structure, Nat. Photonics 6; 591–595.

Holman Z., S. Wolf, C. Ballif, 2013. Improving metal reflectors by suppressing surface plasmon polaritons: a priori calculation of the internal reflectance of a solar cell, *Light Sci. Appl.*, 2: e106-1–e106-6.

Hoppe, H. and N. Sariciftci, 2004. Organic solar cells: an overview, *J. Mater. Res.*, 19, 1924–1945.

Huang L., X. Chen, B. Bai, Q. Tan, G. Jin, T. Zentgraf, S. Zhang, 2013. Helicity dependent directional surface plasmon polariton excitation using a metasurface with interfacial phase discontinuity, *Light Sci. Appl.*, 2: e70-1–e70-7.

Intemann J., K. Yao, Y. Li, H. Yip, Y. Xu, P. Liang, C. Chueh, F. Ding, X. Yang, X. Li, Y. Chen, A.K.-Y. Jen, 2014. Highly efficient inverted organic solar cells through material and interfacial engineering of indacenodithieno(3,2- b)thiophenebased polymers and devices, *Adv. Funct. Mater.*, 24: 1465–1473.

J¨onsson S. M., E. Carlegrim, F. Zhang, W. R. Salaneck, M. Fahlman, 2005. Photo-electron spectroscopy of the contact between the cathode and the active layers in plastic solar cells: the role of LiF, *Japanese Journal of Applied Physics*, 44:3695–3701.

Jo J., J. Pouliot, D. Wynands, S. Collins, J. Kim, T. Nguyen, H. Woo, Y. Sun, M. Leclerc, A.J. Heeger, 2013. Enhanced efficiency of single and tandem organic solar cells incorporating a diketopyrrolopyrrole-basedlow-bandgap polymer by utilizing combined ZnO/polyelectrolyte electron-transport layers, *Adv. Mater.* 25;4783–4788.

Kim K., Y. Kim, W. Kang, B. Kang, S. Yeom, D. Kim, J. Kim, S. Kang, 2010. Inspection of substrate-heated modified PEDOT:PSS morphology for all spray deposited organic photovoltaics, *Solar Energy Materials and Solar Cells*, 94:1303–1306.

Kosten, E., J. Atwater, J. Parsons, A. Polman, H. Atwater, 2013. Highly efficient GaAs solar cells by limiting light emission angle, *Light Sci. Appl.*, 2; e45-1– e45-6.

Krebs, F. 2009. Fabrication and processing of polymer solar cells: a review of printing and coating techniques, *Sol. Energy Mater. Sol. Cells*, 93; 394–412.

Lai Y., Y. Lan, T. Lu, 2013. Strong light-matter interaction in ZnO microcavities, *Light Sci. Appl.*, 2:e76-1–e76-7.

Li, G., V. Shrotriya, J. Huang, Y. Yao, T. Moriarty, K. Emery, Y. Yang, 2005. High- efficiency solution process able polymer photovoltaic cells by self-organization of polymer blends, *Nature Materials*, 4: 864–868.

Ma, L., J. Liu, Y. Yang, 2002. Organic electrical bistable devicesandrewritablememorycells,*ApplPhys.Lett.*,80, 2997.

Ma, W., C. Yang, X. Gong, K. Lee, A. J. Heeger, 2005. Thermally Stable, Efficient polymer solar cells with nanoscale control of the interpenetrating network morphology, *Advanced Functional Materials*, 15: 1617–1622.

Peumans P., A. Yakimov, S. R. Forrest, 2003. Small molecular weight organic thin-film photodetectors and solar cells, Journal of Applied Physics 93:3693–3723.

Po, R., C. Carbonera, A. Bernardi, N. Camaioni, 2011. The role of buffer layers in polymer solar cells, *Energy Environ. Sci.*, 4: 285–310.

Reyes-Reyes M., K. Kim, D. L. Carroll, 2005. High efficiency photovoltaic devices based on annealed poly (3-hexylthiophene) and 1- (3-methoxycarbonyl)-propyl-1-phenyl-(6,6) C (sub 61) blends, *Applied Physics Letters*, 083503–083506.

Romano S., S. Cabrini, I. Renina, V. Mocella, 2014. Guided resonance in negative index photonic crystals: a new approach, *Light Sci. Appl.*, 3: e120-1–e120-5.

Shrotriya V., G. Li, Y. Yao, C.-W. Chu, Y. Yang, 2006. Transition metal oxides as the buffer layer for polymer photovoltaic cells, *Appl. Phys. Lett.*, 88, 073508.

Su Y., Y. Ke, S. Cai, Q. Yao, 2012. Surface plasmon resonance of layer-by-layer gold nanoparticles induced photoelectric current in environmentally-friendly plasmon-sensitized solar cell, *Light Sci. Appl.*, 1; e14-1–e14-5.

Taylor, T. 2012. Nanofluid-based optical filter optimization for PV/T systems, *Light Sci. Appl.*, 1; e34-1–e34-7.

Yang L., H. Chen, M. Wang, 2008. Optimal film thickness for exciton diffusion length measurement by photocurrent response inorganic hetero structures, *Thin Solid Films*, 516: 7701–7707.

Yang X. and J. Loos, 2007. Toward high-performance polymer solar cells: the importance of morphology control. *Macromolecules*, 40:1353–62.

Yip, H. and A. Jen, Recent advances in solution-processed interfacial materials for efficient and stable polymer solar cells, *Energy Environ. Sci.*, 2 (2012) 5994–6011.

Yongbing, L. 2010. Effects of metal electrode reflection and layer thicknesses on the performance of inverted organic solar cells, *Solar Energy Materials and Solar Cells*, 94: 744–749.

Zhang F. J., D. W. Zhao, Z. L. Zhuo, H. Wang, Z. Xu, Y. S. Wang, 2010. Inverted small molecule organic solar cells with Ca modified ITO as cathode and MoO_3 modified Ag as anode, *Solar Energy Material sand Solar Cells*, 94: 2416–2421.

Zhang F., F. Sun, Y. Shi, Z. Zhuo, L. Lu, D. Zhao, Z. Xu, Y. Wang, 2010. Effect of an ultra-thin molybdenum trioxide layer and illumination intensity on the performance of organic photovoltaic devices, *Energy and Fuels*, 24:3739–3742.

Zhao D., W. Tang, L. Ke, S. T. Tan, X. W. Sun, 2010. Efficient bulk heterojunction solar cells with poly (2,7-(9,9-dihexylfluorene)-alt-bithiophene) and 6,6-phenyl C61 butyric acid methyl ester blends and their application in tandem cells, *ACS Applied Materials and Interfaces*, 2: 829–837.

Zhao G., Y. He, Y. Li, 2010. 6.5% Efficiency of polymer solar cells based on poly (3-hexylthiophene) and indene-C(60) bisadduct by device optimization, *Advanced Materials*, 22 4355–4358.

Zhao Y., Z. Xie, Y. Qu, Y. Geng, L. Wang, 2007. Solvent-vapor treatment induced performance enhancement of poly (3-hexylthiophene): methano fullerene bulk-heterojunction photovoltaic cells, *Applied Physics Letters*, 90: 043503–043504.

Zou J., C. Li, C. Chang, H. Yip, A.K.-Y. Jen, 2014. Interfacial engineering of ultrathin Metal film transparent electrode for flexible organic photovoltaic cells, *Adv. Mater.*, 26: 3618–3623.

****